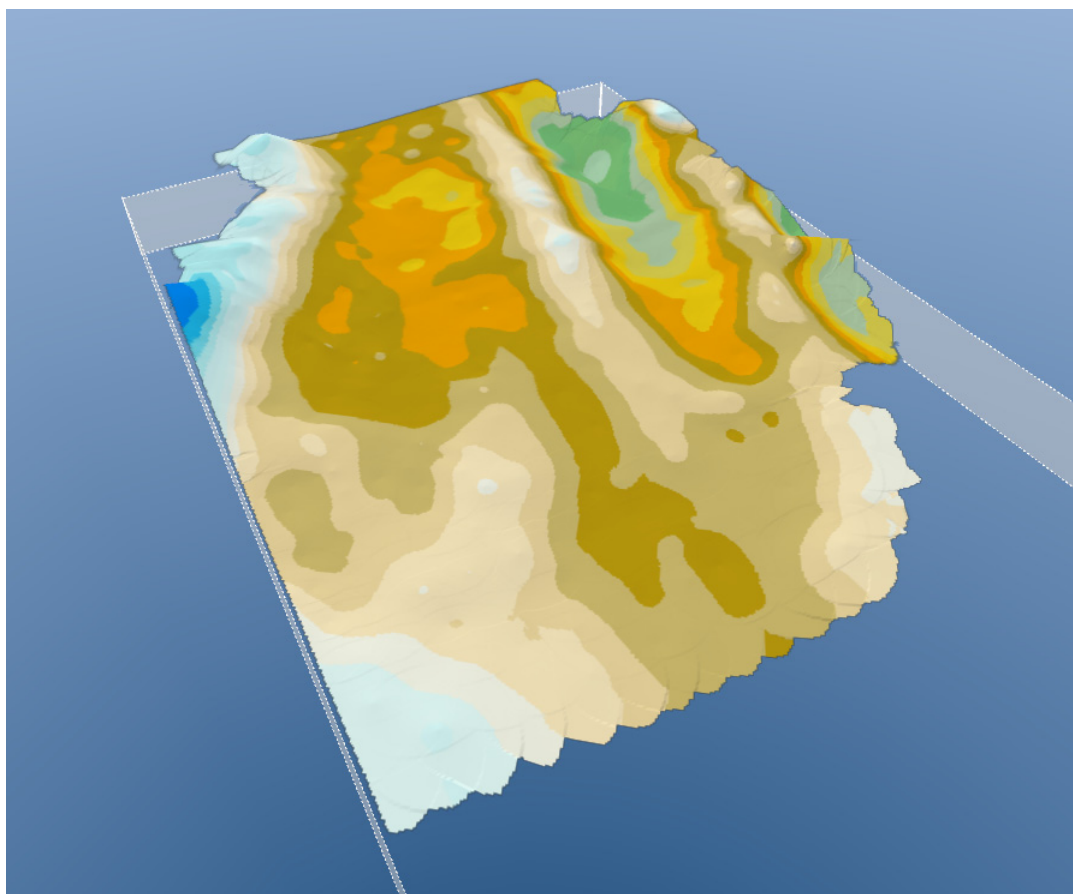


Structural geology of folded terrain in the Rocky Mountains' foothills interpreted from SkyTEM

A preliminary study of SkyTEM data
collected in the Peace region,
NE British Columbia, Canada

Flemming Jørgensen, Antonio Menghini, Anders Juhl Kallesøe, Giulio Vignoli,
Andrea Viezzoli & Stig A. Schack Pedersen



Introduction

GEUS has been invited to carry out an interpretation study within the Peace-project based on data delivered by SkyTEM ApS to Geoscience BC. The Peace Project is a collaborative effort involving the Ministry of Forests, Lands and Natural Resource Operations, the Ministry of Environment, the BC Oil and Gas Commission, the Ministry of Natural Gas Development, BC Oil and Gas Research and Innovation Society (BC OGRIS), Progress Energy Canada Ltd., and ConocoPhillips Canada, with additional support from the Peace River Regional District and the Canadian Association of Petroleum Producers. The authors of this report acknowledge the in-kind and funding support these partners have made to this study, through their contributions to the Peace Project. We also thank the Danish “Market Development Fund” who, in this work, supported the testing of the Smart Interpretation tool through the “Geological modelling of large areas” (GOMILA) project. The SkyTEM data were collected in 2015 using a SkyTEM 312^{Fast} airborne geophysical system and this portion of the survey (referred to as the Main Area in Aarhus Geophysics’ Report 2016-09a) covers a total of approximately 4,000 line-km in northeast British Columbia, Canada. The studied area is a subset of a much larger survey area in which a total amount of 21,000 line-km has been collected (Figure 1). The data have been processed and inverted by Aarhus Geophysics ApS.

The purpose of this interpretation study is to show what can be achieved from the electrical resistivity model obtained by inverting the SkyTEM data, with specific regard to understanding the 3D structural geology within the area. The interpretations are carried out almost without support from additional data. The only supplementary data used are shallow well log data, with only very limited information. We expect that the interpretations could be clearly improved if they were supported by e.g., stratigraphical borehole data, logging data or seismic data. The present report therefore provides some general interpretations of the bedrock geology only, while focus has not been put on the glacial drift deposits.

Follow-ups on this preliminary study will definitely benefit from: (i) the inclusion of additional ancillary data, and (ii) further interaction between geologists and geophysicists aiming at incorporating supplementary geological knowledge into the geophysical inversion, and, in this way, at resolving possible ambiguities in the resistivity models.

Sketches of geological interpretation have been drawn on selected cross sections (flight lines) and on horizontal slices. Furthermore, one single layer boundary has been selected for 3D modelling.

This report describes the interpretation and modelling of SkyTEM data applied to a regime affected by gentle to moderate deformation superimposed by glacial drift sediments of various thickness.

Survey area

The Peace River area is located along the western edge of the Alberta Plateau within the Interior Plains. The topography consists of a series of rolling plateaus and northeastward sloping plains, with a well-developed dendritic drainage system tributary to the Peace River. These secondary valleys are deeply incised. In general, the upland terrain south of the Peace River shows greater relief with respect to the area north of the river.

To the north of the survey area the Sikanni Chief and the Buckinghorse rivers follow a west-east oriented pattern, similar to the Peace River. On the contrary, most of the tributaries of the Peace River flow from NNW towards SSE.

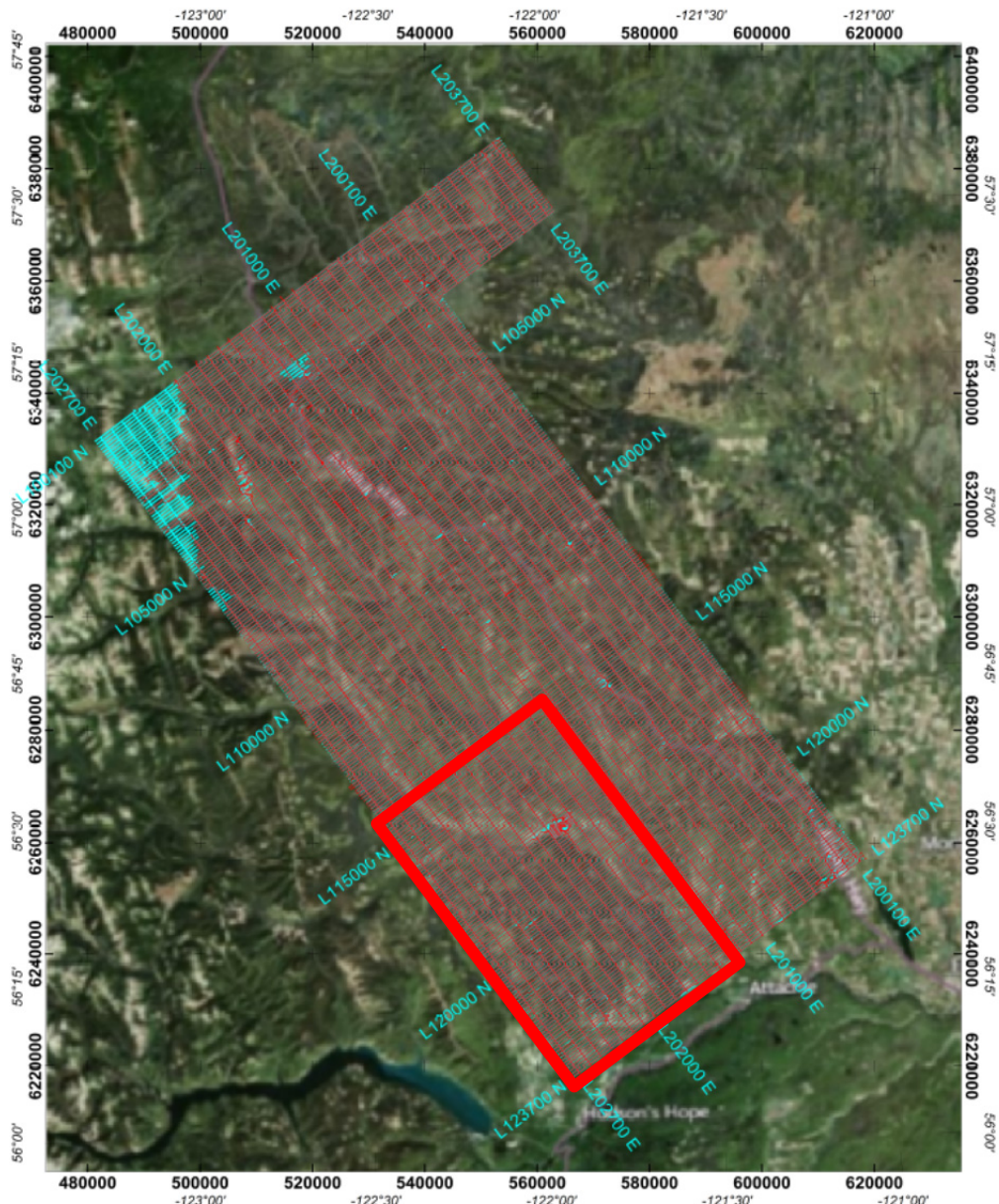


Figure 1: Flight lines of the entire Peace Project survey area (from SkyTEM Surveys ApS, 2016). The area studied in this work is marked by the red rectangle (35 x 56 km).

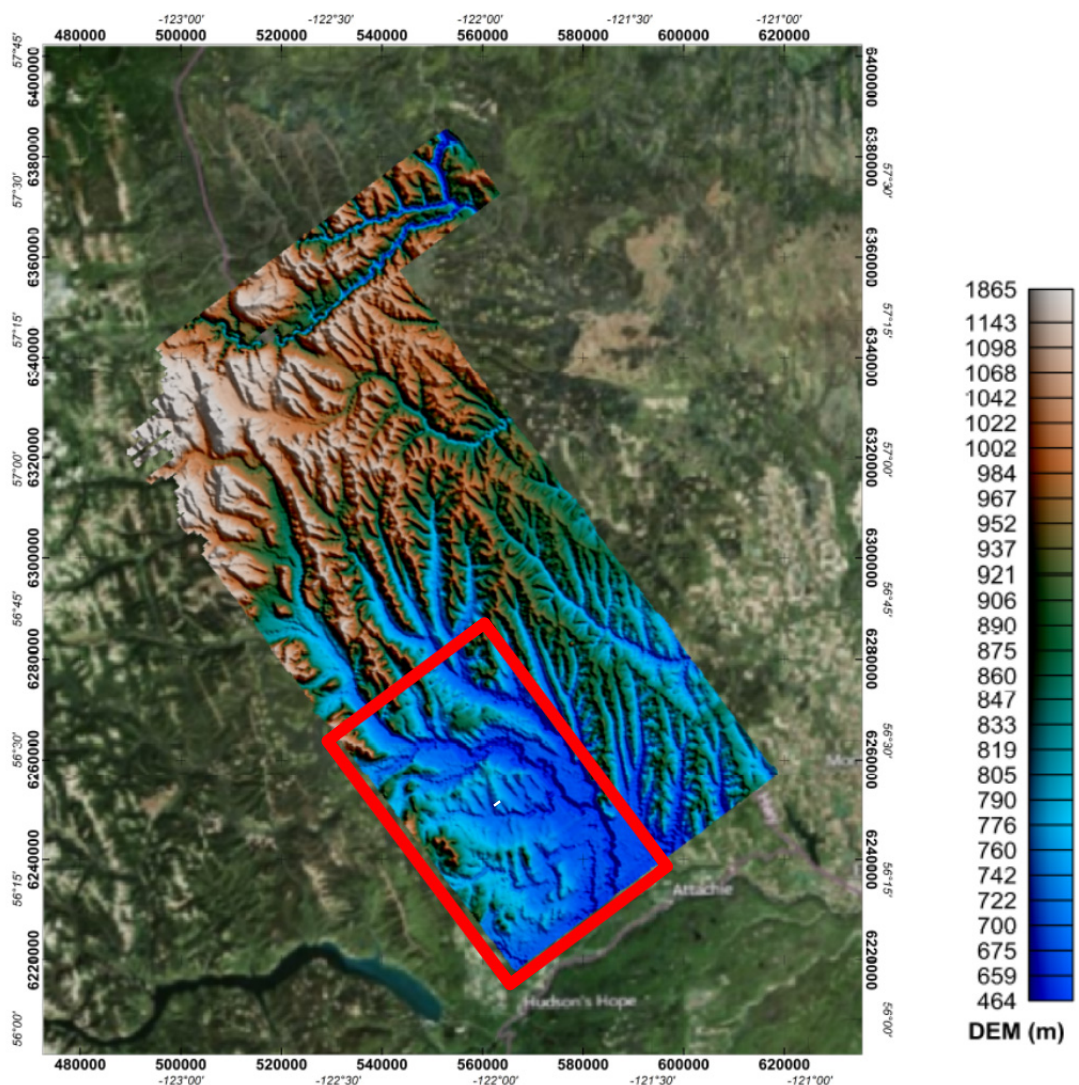


Figure 2: Topographical map of the entire SkyTEM survey area (from SkyTEM Surveys ApS, 2016). The area studied in this work is marked by the red rectangle (35 x 56 km).

Regional geological setting

The study area is situated in the Peace Region, NE British Columbia delimited by the Buckinghorse river (to the north) and by the Peace River (to the south), involving an area of about 1960 km². The flight lines of the survey are oriented NNE-SSW with perpendicular tie lines. The area covered is 35 km wide and 56 km long. The topography is typical for the Rocky Mountains Foothills: dominated by gentle hilly plateaus elevated to 6–700 m a.s.l. and incised by glaciofluvially eroded valleys and recent drainage streams.

The geological setting of the area is dominated by the position between the Cordillera Orogenic Belt to the west, which created the Rocky Mountain Fold Belt, and the Alberta Foreland Basin deposited on the depressed Laurentian craton to the east. In the Rocky Mountain Fold Belt, to the west, sedimentary rocks of younger Palaeozoic and Mesozoic age are exposed in folds and thrust features. The general décollement surface for this deformation is regarded to be situated in the clayey units of upper Devonian and Carboniferous sedimentary rocks. The décollement surface is interpreted to continue into a blind thrust below the foot hills to the east, where the deformation is reduced towards the Alberta Foreland Basin. Sedimentary rocks are here relatively flat, lying under the unconformity between the uppermost Cretaceous clastic sediments and the Quaternary, mainly glacigenic deposits.

In the foreland region, however, it is significant that the Cretaceous rocks are gently folded and displaced by shallow dipping thrust faults dipping towards the east. The interpretation of the décollement surface for this “foot hill” deformation indicates that it is located in clay rich lithologies in the Lower Cretaceous. According to the stratigraphy of the nearby areas (Hinds & Spratt 2005), the Buckinghorse Formation (upper Lower Cretaceous Albian in age) is a good candidate for hosting the décollement zone. This unit was deposited during highstand systems tract. During the regressive system tract the Sikanni and Sully Formations were deposited in the beginning of the Cenomanian. These formations are characterised by greenish and grey, fine-grained lithologies including siderite concretions. During a lowstand systems tract, the Dunvegan Formation was deposited. This formation is dominated by coarse-grained sandstones typically for shallow marine conditions. The Dunvegan Formation constitutes the uppermost bedrock in the area of focus.

The glaciodynamic development during the Quaternary time is ruled by the formation of ice sheets covering the Rocky Mountains to the west and the ice sheets spreading over the Laurentian platform from the east. It mainly consists of units deposited during the last Wisconsinan Glaciation and that are preserved in the region (Hartman & Clague 2008). The depositional environment is strongly influenced by the drainage system created between the margins of the two ice sheets. Records of till beds indicate at least two ice advances from the Cordilleran range and three to four advances from the north-easterly source area (Laurentide Ice Sheet). The drainage from the ice margins resulted in a number of glaciofluvial deposits filling tunnel valleys as well as pro-glacially incised meltwater channels and valleys. However, a more spectacular occurrence is the deposition of sediments in ice dammed lakes. These glaciolacustrine deposits may be more than 100 m thick, and in general they will be cross-cut by glaciofluvial gravel deposits mirroring the discharge of the water in the lakes, when the blocking glaciers withdraw.

The Postglacial to modern development of river systems drained from the mountain range barrier towards the foreland to the east. Due to glacio-isostatic uplift the drainage additionally turned southwards away from the uplift centre.

In the study area, the lithostratigraphical formations that are within the expected penetration depths of the SkyTEM method (2-400 m) are, from below: (i) the Buckinghorse Formation, then, upon this, (ii) the Sikanni Formation, (iii) the Sully Formation and finally topped by (iv) the Dunvegan Formation - e.g., Hinds and Cecile (2003) (Figure 3).

The Buckinghorse Formation is composed by shales, silty mudstones and siltstones. The Sikanni Formation is more heterogeneous, as it is composed by alternating layers of sandstone, siltstone and shale. According to a few electrical logs provided by Geoscience BC, the Sikanni Formation has a resistivity level of 15-20 ohm-m. The Sully Formation is more homogeneous and is composed of mainly shales and siltstones giving it a stronger conductive response in the electrical logs (usually 10-15 ohm-m). However the lower portion can show a bit higher resistivity, close to that one of the Sikanni Formations. The Dunvegan Formation is mainly composed of sandstone with subordinate conglomerates. The sandy facies show higher resistivities in the electrical logs (25-50 ohm-m), while local decrease in resistivity is due to silty shale layers (15-20 ohm-m). It must be noticed that the above-mentioned resistivity values are only inferred from a few electrical logs in a limited part of the survey area. Also, it should be kept in mind that specific resistivity levels measured in electrical logs cannot be directly compared with resistivity levels retrieved from calibrated TEM data.

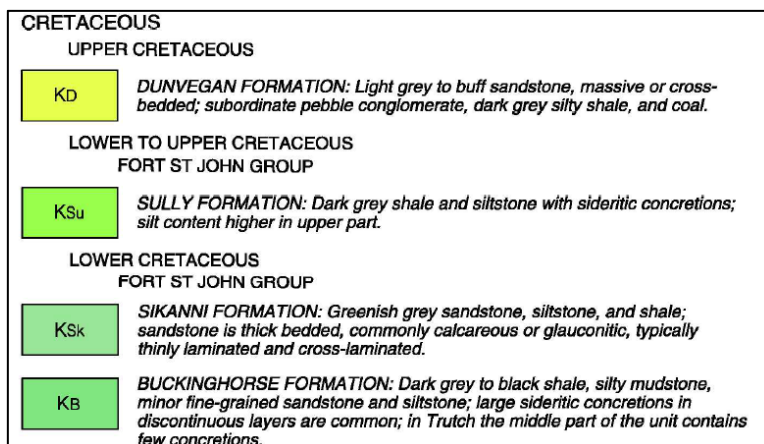


Figure 3: Stratigraphical formations seen in the data within the survey area (from Hinds and Cecile 2003).

Method – the SkyTEM system

The SkyTEM system (Figure 4) is a helicopter time-domain electromagnetic (TEM) system specifically designed for hydrogeological, environmental and mineral exploration. It is operated with an external sling load independent from the helicopter. The transmitter is characterized by a dual-moment system with a maximum magnetic moment of approximately 490.000 Am^2 . Two lasers measure continuously the distance from the frame to the terrain, and two inclinometers measure the tilt. Power is supplied by a generator placed between the helicopter and the frame.



Figure 4: SkyTEM 312^{Fast} system.

Data

SkyTEM data

A total of about 4,000 line-km of SkyTEM data were acquired in the study area (Figure 5). There is 600 m between SW-NE flight lines and 2400 m between NW-SE flight lines. The data were carefully processed and noise affected data were culled. After processing, Aarhus Geophysics ApS applied a (quasi-)3D Spatially Constrained Inversion (SCI) with a vertical parametrization of 30 layers in order to infer the electrical resistivity distribution.

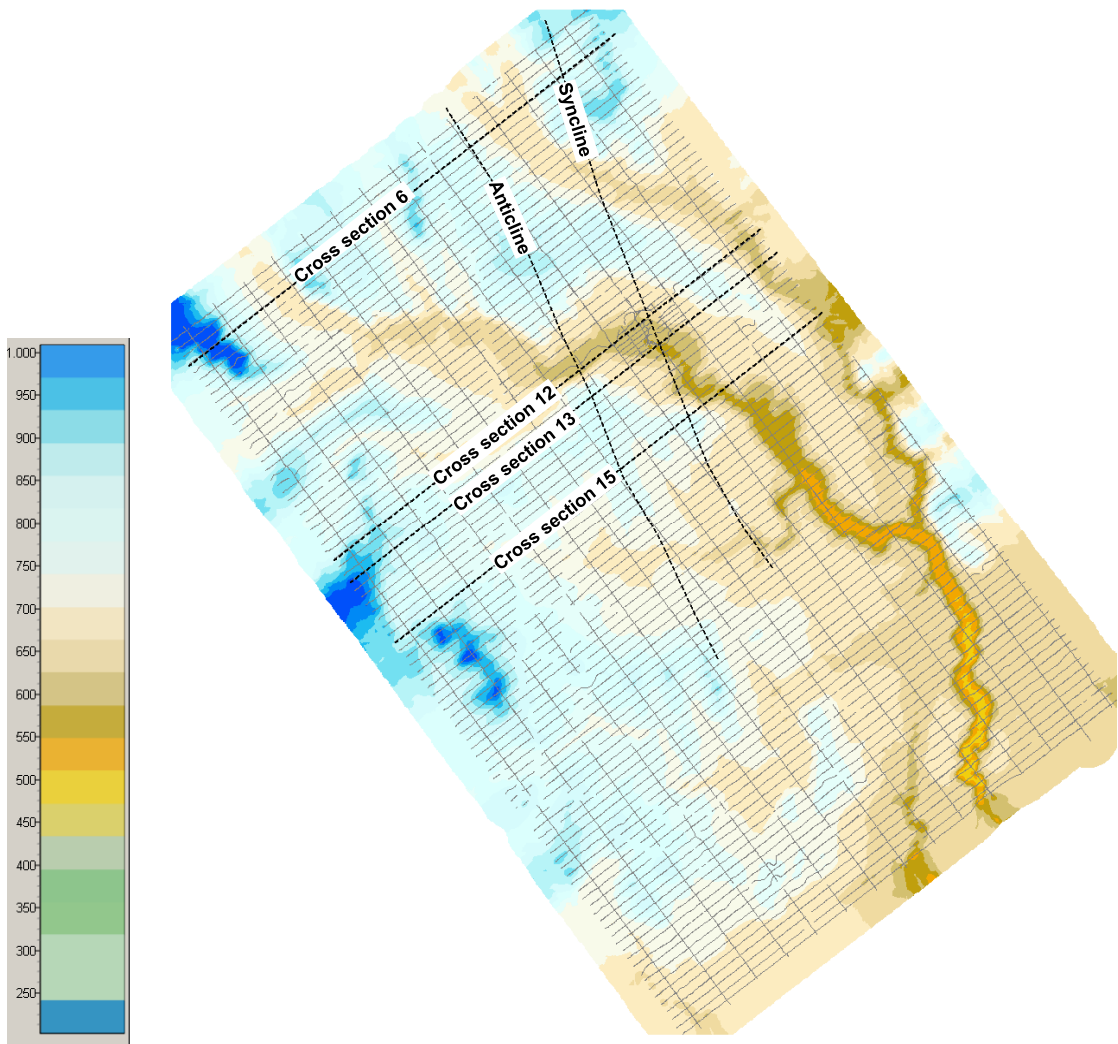


Figure 5: Post-processed data within the study area. Flight line spacing is 600 m between SW-NE lines and 2,400 m between NW-SE lines. The area is in total app. 35 x 56 km. Topographical map shown in background and locations of cross sections are shown.

SCI provides a full non-linear damped least squares solution in which the transfer function of the instrumentation is modelled. The modelization includes, among other things, current turn-on and -off ramps, front gate and low pass filters, system altitude, etc. The inversion kernel is “AarhusInv”, developed at the University of Aarhus. This code performs efficient large-scale inversions and is crucial for testing inversions as well as examining the model space. Within the SCI’s framework, the inherent ill-posedness of the inversion is tackled by enforcing some degree of continuities between neighbouring resistivity values (in both ver-

tical and horizontal directions). In this way, the smoothest resistivity model among all the possible solutions compatible with the data is selected.

In turn, the resistivity inversion result has been interpolated into a 3D resistivity grid. Geological interpretations are based on this grid and most interpretations are performed on cross sections through the grid along flight line locations. In some cases, however, interpretations are also done on cross sections drawn across/along specific geological features.

Resistivity values are shown by using a dedicated scale, where blue colours represent low resistivities, and red and pink colours show high resistivities (Figure 6).

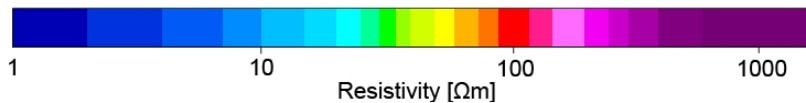


Figure 6: Resistivity colour scale

Borehole data

Some boreholes (provided by Geoscience BC and describing depth and type of bedrock) were inspected and used for comparison with resistivities on the vertical cross sections. Unfortunately, the stratigraphic data regarding the glacial drift were absent, and they were only used to assess the resolution of the Quaternary deposits thickness and the nature of the bedrock.

The lithological logs of the boreholes are drawn on the presented cross sections (below) with the legend shown in Figure 7.

Borehole legend:



Figure 7: Borehole legend used on cross sections in figures below.

Geological interpretation of the SkyTEM data

Cross sections

From the SkyTEM data acquired in the Peace Region, a large number of cross sections have been constructed, among which we present here four illustrative and representative selections. The location of the cross sections is shown in Figure 5. Estimated thrust faults are delineated with thick black lines and inferred layer boundaries are delineated by thinner black lines.

The first cross section is from the northern part of the area (Figure 8). At the base of the cross section a thick unit of medium to low resistivity is recognized. The base of this unit is in the central part of the cross section apparently located at a depth of 350 – 400 m a.s.l. The thickness, however, is very uncertain since the depth of investigation (DOI) is hardly deep enough to really detect the base of the unit. Towards the west, the unit is repeatedly elevated due to thrust faulting. The medium- to low-resistive unit is interpreted as a clay-rich succession corresponding to the Buckinghorse Formation deposited during the high stand system in the middle Cretaceous. Above this unit, an up to 150 m thick resistive unit is recognized. This is interpreted as the Sikanni Formation where the sandy intercalations in silt and clay beds make the unit more resistive compared to the Buckinghorse Formation. It was probably deposited during the regressive systems tract during depositional fan-building-out towards a pro-delta environment. This type of setting may well explain the variation in thickness of the Sikanni Formation (Figure 8). At the top of the Sikanni Formation a more conductive unit of up to 100 m occurs. This unit is interpreted as clay-rich lagunal deposit corresponding to the Sully Formation. The variation in thickness is mainly due to variations in topography. Meanwhile, features with very high resistivities are present at some of the highest peaks above the Sully Formation. Those can be interpreted as remnants of the sandy Dunvegan Formation deposited during low stand systems tract.

The main structural features dominating Cross section 6 (Figure 8) are the anticline and syncline in the middle part, and the thrust fault deformation to the west (left). The anticline (at 23,000 m) is a key structure, which will be traced in the following cross sections and horizontal slices. Northeast of the anticline (to the right) only the western limb of an open syncline is distinguishable. Note that a tunnel-valley up to 150 m deep was eroded into the syncline, an obvious location for superposed erosion in a pre-existing depression. The valley may have developed into an ice-dammed lake, in which clay-rich glaciolacustrine sediments were deposited - indicated by the conductive unit in the valley.

In Cross section 12 (Figure 9), the key anticline is situated at 20,000 m. Note that in this cross section the Buckinghorse Formation crops out at the crest of the anti-cline, and the Sikanni Formation forms the cover unit in the crest zone. A borehole right in the crest zone confirms the occurrence of the Buckinghorse Formation here. The increase in resistivity in the deepest part of the section is probably due to a decreasing clay content of the Buckinghorse Formation. The boundary shown with a broken line in Figure 9, Figure 10 and Figure 11 is therefore most likely an internal boundary within this formation. Thus, the thickness of the Buckinghorse Formation is unknown.

The syncline to the northeast (to the right) is relatively well outlined, mainly by the more resistive unit interpreted as the Sikanni Formation. The thrust faults ramping up at the base of the cross section are regarded to be part of the detachment folds. The final displacement along the thrust fault to the southwest (right) is responsible for the outcrops of the Buckinghorse Formation in the elevated position of about 900 m a.s.l. Note that the boundary between the Sikanni and Sully Formations is in some places truncated by thin horizontal units of both low and high resistivity. These could be interpreted as glaciofluvial terraces deposited during various steps in the drainage pattern of discharging river systems during the termination of the Wisconsin Glaciation.

In Cross section 13 (Figure 10), the Sikanni Formation is seen to clearly outline the key anticline (at 19,500 m) as well as the north-eastern syncline (at 25,000 m). The key anticline with the Sikanni Formation is actually forming a hill. In the north-eastern syncline (pro-glacial), river erosion has formed a wide valley. Prior to this valley erosion, shallow, sub-horizontal units of high and low resistivity indicate phases of glaciofluvial outwash plain formation.

The last cross section to be presented here is Cross section 15 (Figure 11). The key anticline has here changed from a nearly tight limbed anticline (in the other cross sections) to an open folded anticline with shallow dipping limbs. In the syncline to the east the glaciofluvial terraces in the river system are very marked. The Buckinghorse Formation is almost exposed to the south-west (left) due to the lift by a thrust fault ramp. The flattening of the fold structures is probably due to an increase in displacement along the south-western ramping thrust fault.

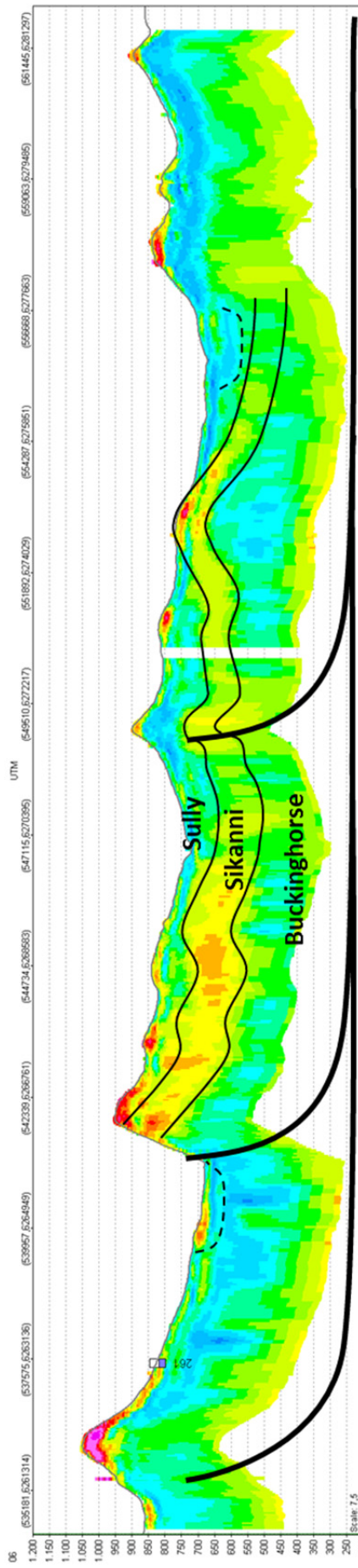


Figure 8: Cross section 6. The three main formations identified are indicated. The interpreted décollement surface is not verified by other investigations, but based on the outlined structures its existence is inferred. Left is southwest and right is northeast. Vertical exaggeration: 7.5x.

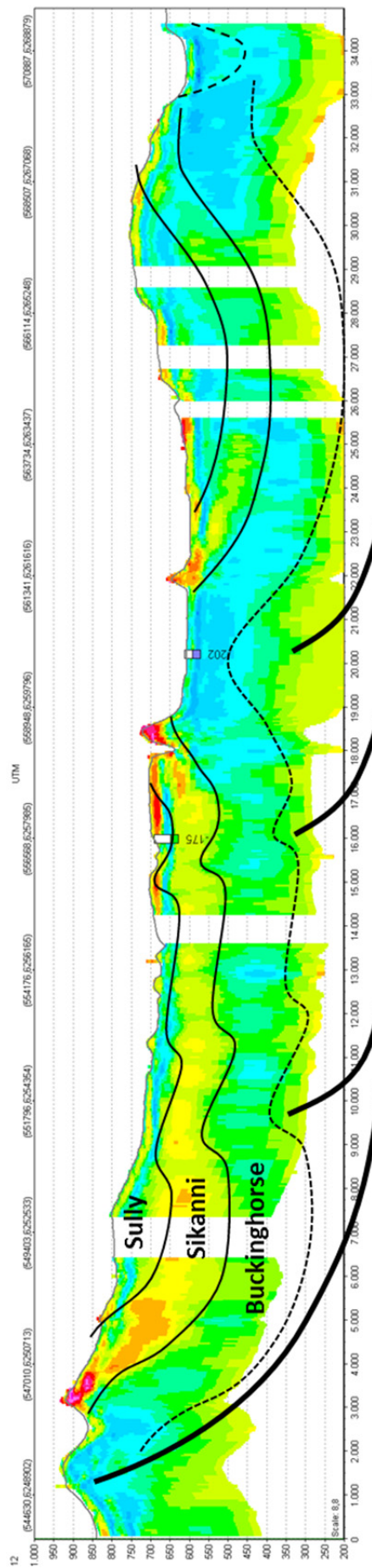


Figure 9: Cross section 12. In this cross section the key anticline is seen at 20,000 m. Note that the Buckinghorse Formation crops out in the crest of the anticline. Furthermore, the Buckinghorse Formation crops out on the top of the thrust sheet displaced along the southwestern, moderately NE-dipping ramp (at 2,000 m). Vertical exaggeration: 8.8x.

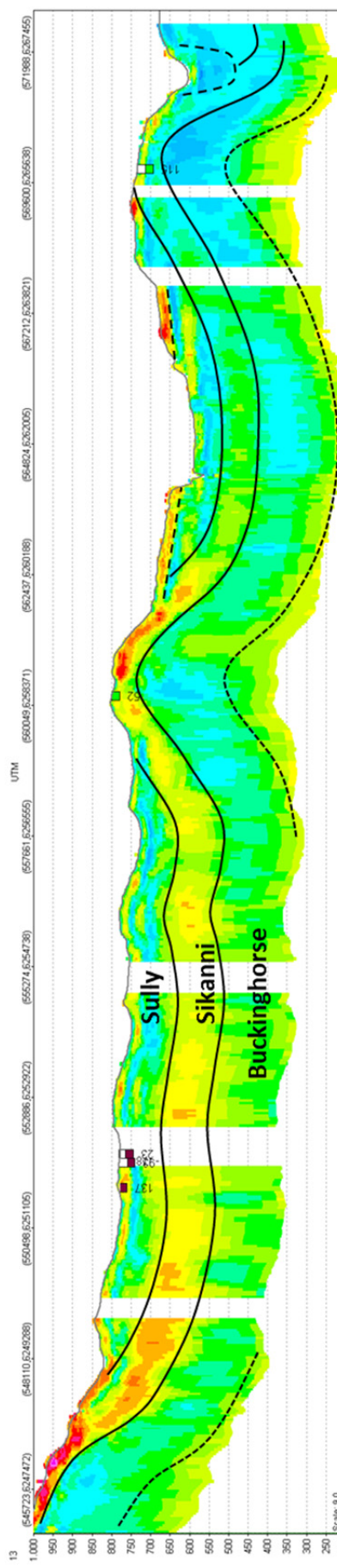


Figure 10: Cross section 13. The key anticline (at 19,500 m) is here encapsulated by the Sikanni Formation. In the syncline to the northeast (at 25,000 m) a proglacial river valley developed followed by phases of glaciofluvial outwash plain formation. The décollement surface and thrust faults are not interpreted in this cross section. However, it is evident that the south-western (to the left) thrust-fault ramp exists, which brings the Buckinghorse Formation up to the highly elevated position of about 1,000 m a.s.l. Vertical exaggeration: 9x.

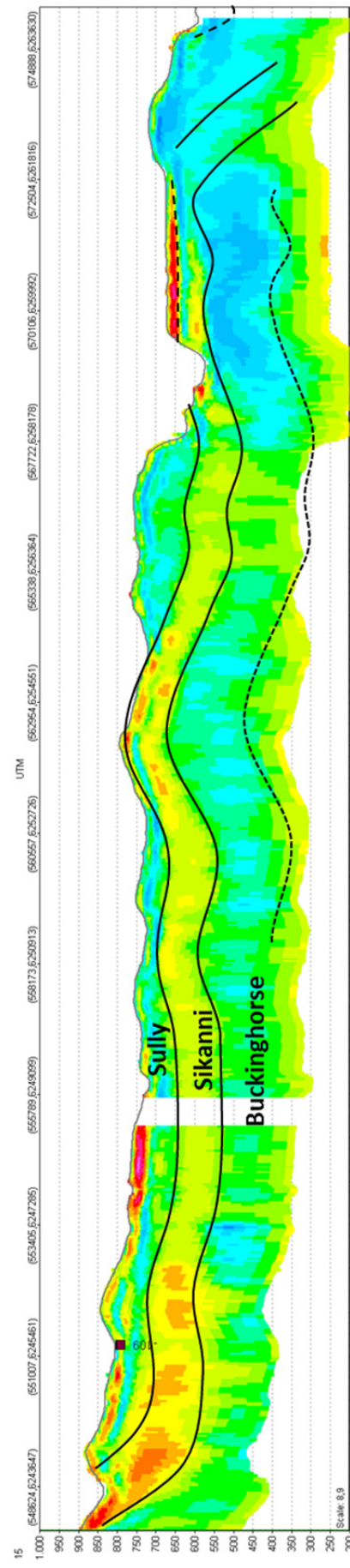


Figure 11: Cross section 15. The key anticline has turned into an open fold with gently dipping limbs. To the south-west (left) the Buckinghorse Formation is continuously lifted up by the westerly verging thrust faulting. Vertical exaggeration: 8.9x.

Geological interpretation of horizontal slices

Three horizontal slices have been chosen to illustrate the interpretations of the structural geology (Figure 12). The slices demonstrate the geometric development of the folded structures. The vertical distance between the slices is 70 m and it is clearly seen that the distance between the limbs in the central key anticline increases with depth.

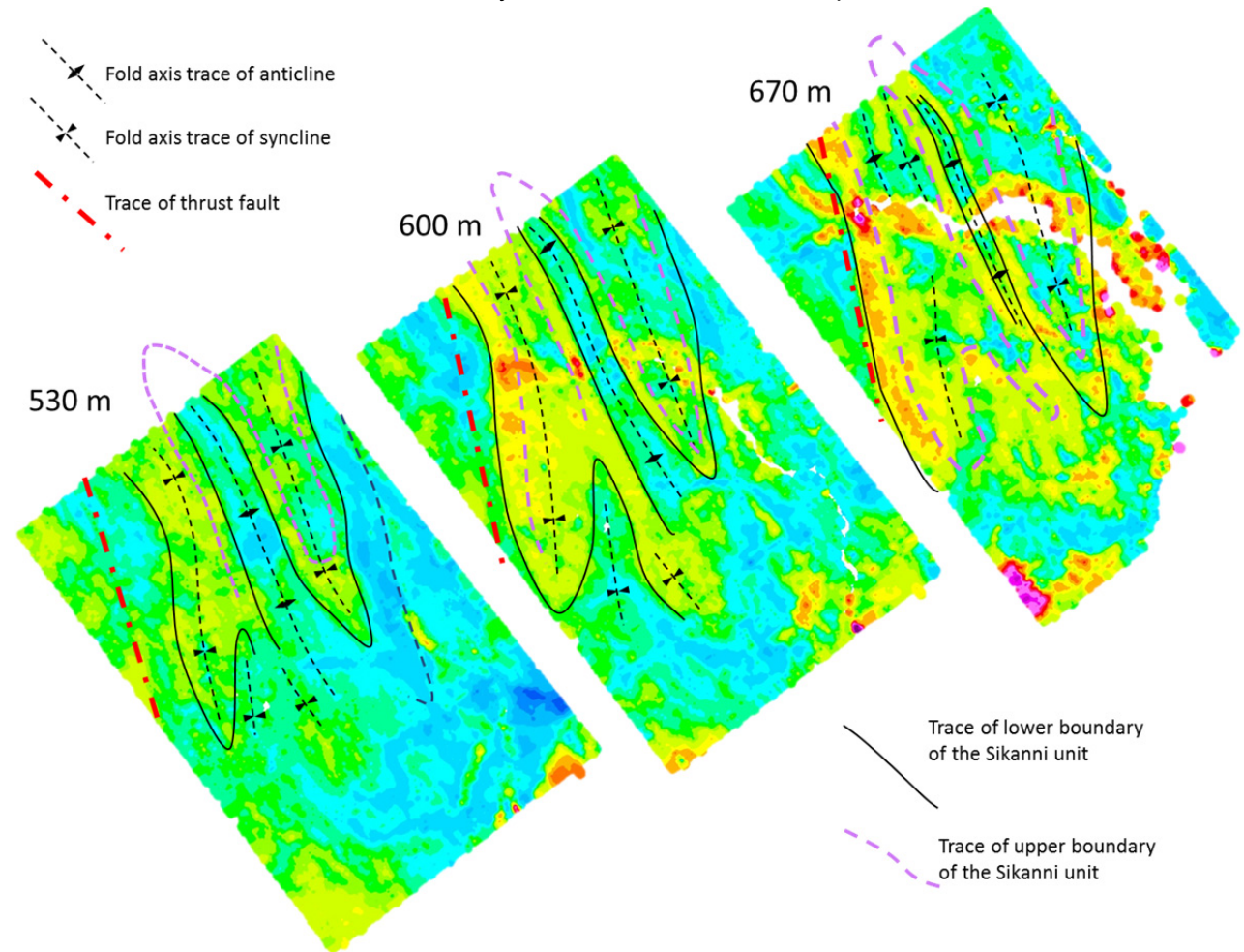


Figure 12: Three depth slices with interpretations showing the folded structures separated by a vertical distance of 70 m. Note how the distance between the limbs in the central anticline increases due to increased depth.

Another marked feature popping up from the horizontal slices is that the fold axes of the anticline and the north-eastern syncline converge. To analyse the structures in more detail, a cross section was therefore constructed along the axis of the syncline (Figure 13) and another was constructed along the axis of the key anticline (Figure 14). The plunge of the north-eastern syncline can be measured to about 3° to the NNW (Figure 13), whereas the plunge of the fold axis in the key anticline is between 1° and 2° to the SSE in the southern part of the area (Figure 14). Meanwhile, the detailed analysis of the plunge of the fold axis in the key anticline demonstrated that the fold axis of the anticline was culminating in the central part of the area. The fold axes therefore plunges in the same direction as the syncline (NNW) in the north-eastern part of the area.

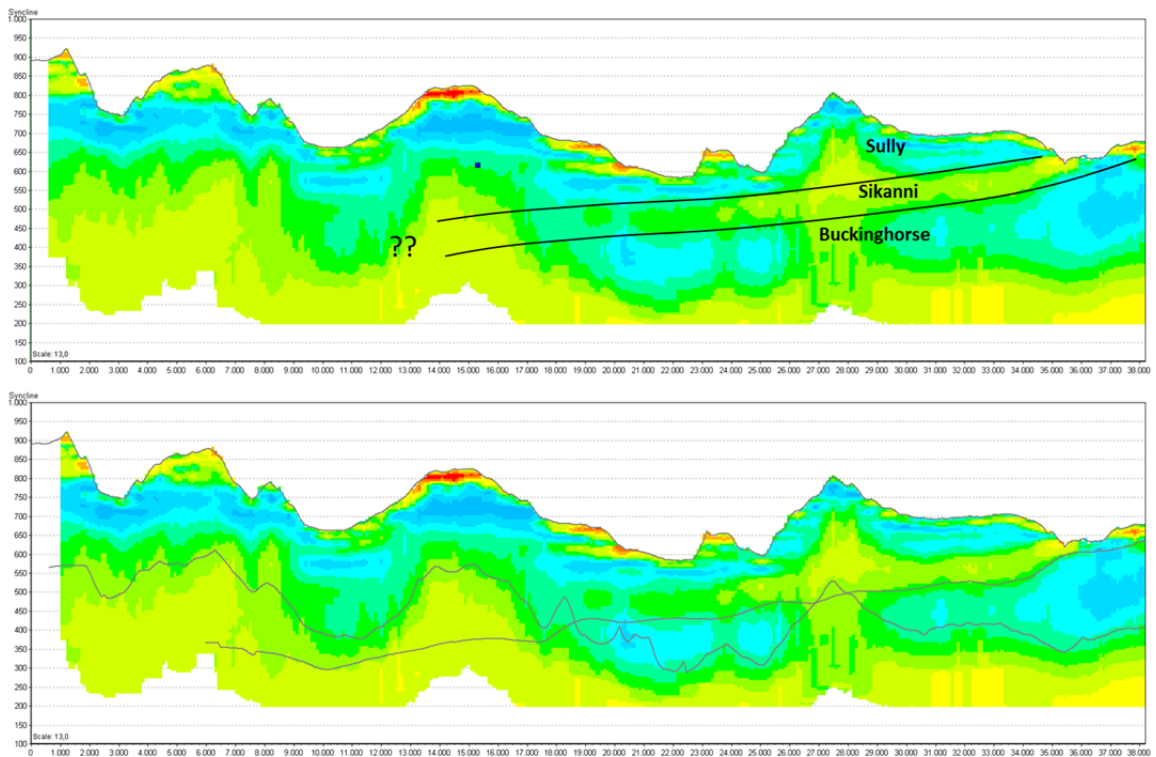


Figure 13: Cross section along the fold axis of the north-eastern syncline (left is NNW, right is SSE). Upper panel: with interpretation of Sikanni. Lower panel: Calculated depth of investigation (DOI - conservative) and 3D model boundary. It is seen that the Sikanni Formation cannot be traced in the northern part of the section, since it is situated deeper than the DOI. The plunge of the fold axis is about 3° to the NNW. Vertical exaggeration: 13x.

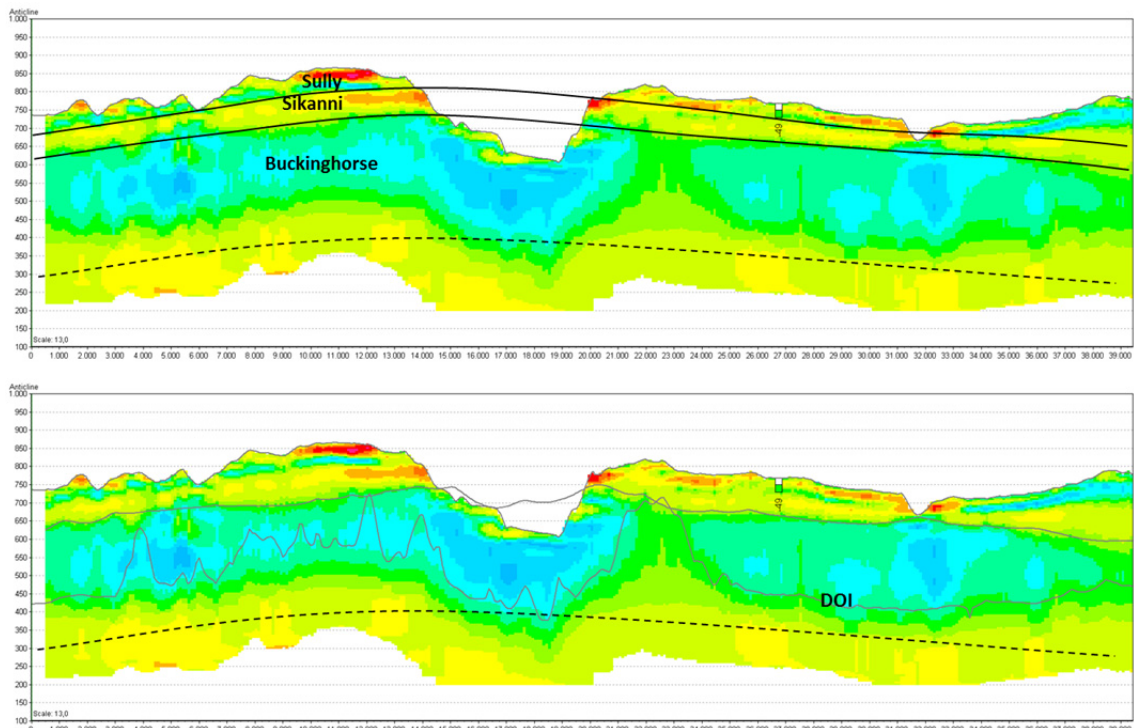


Figure 14: Cross section along the fold axis of the key anticline. Upper panel: with interpretations. Lower panel: calculated depth of investigation (DOI - conservative) and 3D model boundary. Note that according to the DOI there is almost no information of the lower boundary of Buckinghorse (shown with broken black line). This cross section demonstrates the culmination of the fold axis. The plunge of the divergent fold axes is documented by the well-defined boundary between the Buckinghorse Formation and the Sikanni Formation. Note the coinciding location between the culminating fold axis and the deep erosion of the river valley. Vertical exaggeration: 13x.

3D geological model

The lower boundary of the Sikanni Formation has been modelled by applying interpretation points in the 3D model software GeoScene3D (I-GIS) (Figure 15). The modelling was partly conducted by using the newly developed Localized Smart Interpretation routine (Guldbrandsen et al. submitted). The interpretation of the surface is predominantly based on the prepared 3D resistivity grid of the inverted SkyTEM soundings. The northwestern syncline axis dips down to approx. 300 m a.s.l. in the study area. The anticline axis is found at elevations above 700 m a.s.l.

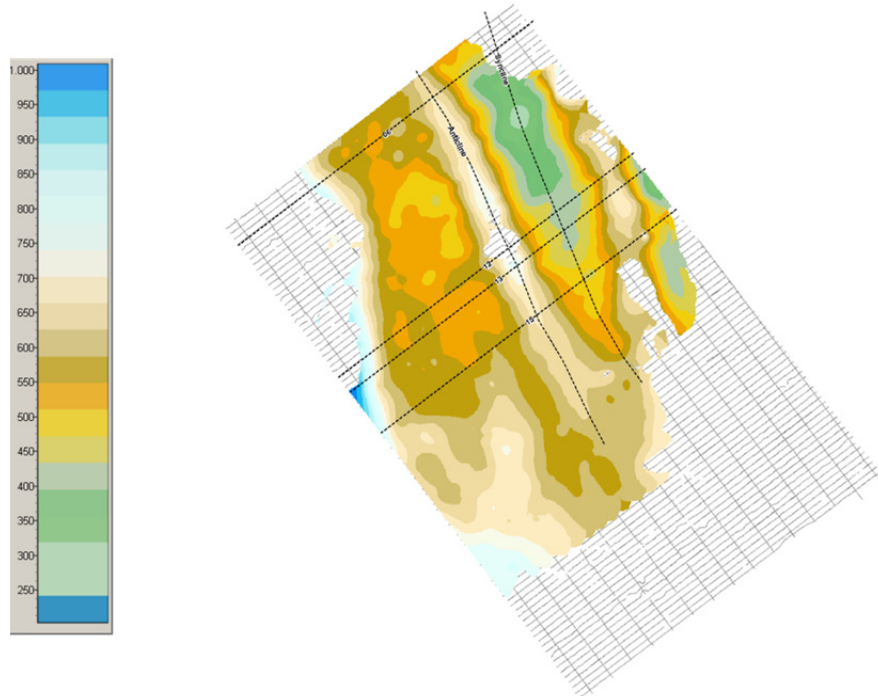


Figure 15: 3D model of the Sikanni Formation, lower boundary (blanked at ground level)

Figure 16 shows a 3D view from the South of the modelled surface.

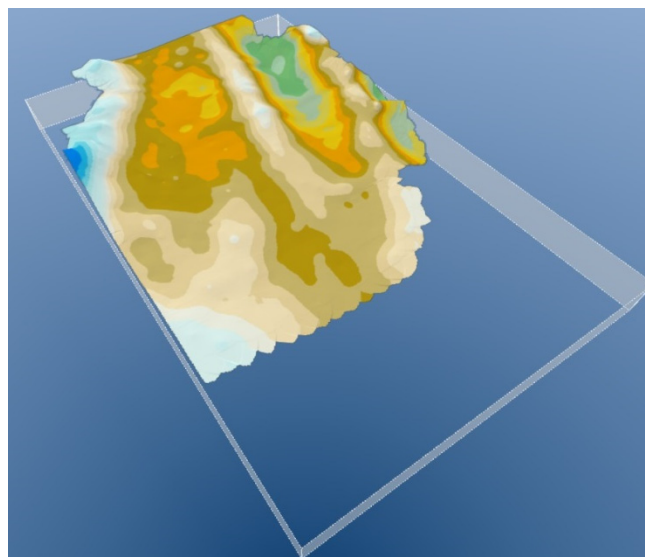


Figure 16: 3D view from the South showing the modelled lower boundary of the Sikanni Formation.

Discussion

This work has been performed solely based on SkyTEM EM data. We have only used very poor and shallow borehole data in a few places. These borehole data are used for the overall stratigraphical subdivision of layers represented in the resistivity data, but their spatial variations are not informed by the borehole data. With more and better borehole data (and other ancillary information) at hand, the interpretations can be improved. For instance, it would be possible to characterize the resistivity variations of the stratigraphical layers in more detail, and, in turn, this would increase our ability to locate the layer boundaries more precisely during interpretation and modelling. Since the layers we interpret and model are not lithostratigraphical units, they vary in clay content both vertically and horizontally. Thus, they will exhibit also variations in resistivity, and sometimes there will be no resistivity contrast between the formations. This means that the formation boundaries cannot always be continuously detected even if we had been able to make a proper resistivity characterization of the formations.

During our interpretations, we have often come across a conductor, approximately 15-20 m thick and located at about 20-25 m below terrain. This layer, of unknown geological, geochemical and hydrochemical origin, is difficult to integrate within the current geological model. Further activities, including comparison with ancillary data (e.g., seismic, stratigraphy) and other inversions with different regularizations, will be beneficial to clarify this point. We therefore expect the shallow part of the geophysical modelling to be improvable, and our focus has not been put here yet.

During our work, we have regularly consulted the calculated Depth Of Investigation (DOI). We have used a conservative estimation (Christiansen and Auken, 2012). Since we have no ancillary data for control, we cannot discuss the eventual usability of data below the DOI. It is our impression, though, that some pieces of reliable information are still available below the considered DOI. In general, however, caution has to be taken when the deeper part around and below the DOI is evaluated. The DOI is not shown on most of the cross sections in Fig. 8-11. The deeper parts of the interpretations are therefore much uncertain here (lower boundary of Buckinghorse and the deep thrusts and décollement).

In our structural model, we have suggested a décollement level to be situated in or just below the Buckinghorse Formation. Two arguments support this suggestion: (1) the clay-rich lithology of the Buckinghorse Formation is suitable for thrusting, and (2) the presence of the ramping thrust fault to the west, in which the Buckinghorse Formation is the lowest unit represented in the displaced thrust sheet. It might also be possible that a décollement level exists much deeper, and that the deformation also affected deeper beds. Our data are not able to confirm or deny this. However, the thin-skinned thrust-fault model presented provides a reasonable match to the data available.

Summary and proposal for future work

GEUS has performed an interpretation study on a portion of the SkyTEM dataset within the Peace-project, British Columbia. Based on a dense grid of SkyTEM soundings, a conceptual structural geological model has been developed. Interpretations of formation boundaries are delineated on selected flight-line transects and on horizontal slices. 3D modelling has been applied to one of the boundaries.

The conceptual model presents a sedimentary regime affected by gentle to moderate deformation and thin-skinned thrust faulting. The stratigraphic formations are well resolved in the geophysical data, but, in this preliminary study, we have only controlled our interpretations against other data to a limited degree.

The deformed sedimentary bedrock is superimposed by glacial sediments of various thicknesses. Details within the glacial drift have not been taken into account in this work. Further geophysical inversion including geological background knowledge is expected to improve the near-surface results and we recommend a close, iterative collaboration between geophysicists and geologists for this task.

The interpretations of the selected stratigraphical formations represent a basic structural framework for future property modelling. This framework therefore constitutes a solid basis for 3D lithological/hydrogeological modelling. We propose the following procedure to build a 3D lithological/hydrogeological model for the area:

1. In order to incorporate all possible pieces of information derived by the geological interpretation and to produce a coherent geological/geophysical image, the geophysical data are further investigated in close collaboration between geologists and geophysicist. The geophysical model already provided by Aarhus Geophysics ApS is the starting point of this study. This preliminary model is based on a reasonable and largely accepted assumption of a smoothly varying resistivity distribution. The geophysical model can be further enhanced by including additional constraints derived from the understanding of the geological setting. Such approach consists of a continuous interaction between geologists and geophysicists in order to recover a geophysical reconstruction that concurrently: (i) is consistent with the geological understanding and conceptual model, and (ii) fits the geophysical data within the noise level. Following this iterative approach GEUS has, together with Aarhus Geophysics ApS, already started to investigate (for specific subareas) alternative geophysical results obtained by using different (e.g., sharp) regularization constraints that seem to better match the geological assumptions put forward.
2. Detailed interpretation of the whole data set (including the shallow part) is performed. All ancillary data and information are now included. A conceptual geological model is completed.
3. The conceptual geological model is the basis for the construction of the 3D lithological/hydrological model. This 3D model is built as a voxel model with lithofacies and/or lithology as first level property. If information about hydraulic parameters is available from borehole data, associated voxel properties can be e.g. hydraulic

conductivity, transmissivity or aquifer potential. For property distribution and spatial voxel constraining, dedicated semi-automatic modelling procedures are conducted. For this work and for the construction of layer boundaries the newly developed multiple point simulation tools and Localized Smart Interpretation technique, both implemented in GeoScene3D, will be beneficial to apply.

We believe that the proposed approach for 3D lithological/hydrogeological modelling could also be beneficial to apply to the entire Peace Project SkyTEM survey, beyond the subset analysed here.

References

- Christiansen, A.V. & Auken, E. 2012: A global measure for depth of investigation. *Geophysics* **77**, WB171–WB177.
- Gulbrandsen et. al submitted: Localized Smart Interpretation - Automatic geological interpretations based on supervised statistical models" submitted to Computational Geosciences.
- Hartman, G.M. & Clague, J.J. 2008: Quaternary stratigraphy and glacial history of the Peace River valley, northeast British Columbia. *Can. J. Earth Sci.* **45**, 549–564.
- Hinds, S.J. & Cecile, M.P. (a.o.) 2003: Pink Mountain and northwest Cypress Creek Map areas (94G/2 & NW94B15), scale 1:50 000. Open file geological map, Geological Survey of Canada.
- Hinds, S.J. & Spratt, D.A. 2005: Stratigraphy, Structure, and Tectonic History of the Pink Mountain Anticline, Trutch (94G) and Halfway River (94B) Map Areas, Northeastern British Columbia. *Bulletin of Canadian Petroleum Geology* **53**, 84–98.
- SkyTEM Surveys ApS, 2016: SkyTEM Survey: British Columbia, Canada. Data report